

# 铁催化高压歧化生成的单壁碳纳米管 氢等离子体的微波损耗机理

郭燕春<sup>1</sup> 彭志华<sup>1</sup> 陈铀<sup>1</sup> 贾鹏<sup>1</sup> 彭延峰<sup>1</sup> 宁艳桃<sup>1</sup> 郭萍<sup>1</sup>

## 摘要

运用双流体理论,在同时考虑了单壁碳纳米管中氢等离子体的电子碰撞吸收和氢离子碰撞吸收的基础上,理论推导出了铁催化高压歧化生成的单壁碳纳米管中氢等离子体的微波衰减系数公式,数值计算了0.2~18 GHz频段的微波衰减系数.计算结果表明,铁催化高压歧化生成的单壁碳纳米管中氢等离子体对2.45 GHz的微波产生强烈损耗.理论与实验数据相吻合.

## 关键词

单壁碳纳米管;氢等离子体;复介电常数;微波损耗

中图分类号 TM25

文献标志码 A

## 0 引言

碳纳米管(Carbon Nanotubes, CNTs)是理想的准一维纳米材料,具有良好的吸附储氢性能<sup>[1-3]</sup>.纯碳纳米管对微波的吸收性能较弱<sup>[4]</sup>,而铁催化高压歧化生成的碳纳米管对2.45 GHz的微波产生强烈吸收<sup>[5]</sup>,但其微波损耗机理目前尚无定论.文献[6-7]的实验研究显示,铁催化高压歧化生成的碳纳米管对微波的损耗和H<sub>2</sub>的热活性释放之间有密切联系.2006年,Ye等<sup>[8]</sup>提出了铁催化高压歧化生成的碳纳米管微波损耗的唯象模型.该模型有助于认识碳纳米管受微波场作用的动力学机制,提供了一种理解碳纳米管在微波辐射下产生剧烈热效应的方法.但这种唯象模型主要适用于红外频段,而在微波频段该模型不能解释铁催化高压歧化生成的碳纳米管只对2.45 GHz频率的微波产生强烈损耗的原因.本文同时考虑了单壁碳纳米管中氢等离子体的电子碰撞和氢离子碰撞对微波的损耗效果,运用双流体理论,推导了铁催化高压歧化生成的单壁碳纳米管中氢等离子体的复介电常数和微波损耗系数公式,构建了单壁碳纳米管中氢等离子体微波损耗的理论模型,计算了0.2~18 GHz频段的微波衰减系数.模拟结果显示,单壁碳纳米管中的电子碰撞是微波损耗的主要原因,氢离子碰撞对微波损耗的贡献不是很大,这与文献[9]用微波吸收模型模拟的结果相一致.

## 1 铁催化高压歧化生成的单壁碳纳米管中氢等离子体的复介电常数

研究<sup>[5-7]</sup>表明,铁催化高压歧化生成的单壁碳纳米管具有良好的吸附储氢性能.常温下,其氢吸附量一般可达 $(4.3 \sim 9.0) \times 10^{-3}$ (质量分数)<sup>[10-12]</sup>;当温度降至77 K时,吸附量可增至 $2.5 \times 10^{-2}$ (质量分数)<sup>[12]</sup>.这些被吸附的氢气来源于实验室环境或其中的水和铁催化反应生成的氢气以及吸收的有机物(如作为热解物的溶剂或泵油)<sup>[4]</sup>.

Baldwin<sup>[13]</sup>在散射实验的基础上,对等离子体的热效应,尤其是包括朗道阻尼进行了微观分析,充分证明了等离子体具有介电损耗特性.根据双流体理论<sup>[14]</sup>,把单壁碳纳米管内氢等离子体中的电子和氢离子都作为导电流体来处理,分别考虑它们的运动.设 $\alpha = e, i$ 分别

收稿日期 2011-11-11

资助项目 南华大学研究生科研创新项目(2011XCX04;2010XCX02);湖南省科学研究项目(2010FJ4092);湖南省自然科学基金(重点)(10JJ8005)

作者简介

郭燕春,女,硕士生,主要研究方向为碳纳米管材料的物理特性. gychungye@163.com

彭志华(通信作者),男,博士,副教授,主要研究方向为碳纳米管材料的物理特性. hndxpzh@sina.com

表示电子和氢离子,质量为  $m_\alpha$ ,电量为  $q_\alpha$  ( $q_e = -e$ ,  $q_i = e$ ),平均速度为  $\mathbf{U}_\alpha$ , $\alpha$ 类粒子的数目为  $N_\alpha$ ,并设系统由  $N$  个 ( $N = 2N_e = 2N_i$ ) 带电粒子所构成,体积为  $V$ ,用  $n_\alpha$  和  $\mathbf{P}_\alpha$  分别表示  $t$  时刻在位形空间的  $\mathbf{x}$  点  $\alpha$  类粒子的数密度和压强张量,则系统中各物理量之间满足的连续性方程为

$$\frac{\partial(n_i - n_e)}{\partial t} + \nabla \cdot (n_i \mathbf{U}_i - n_e \mathbf{U}_e) = 0, \quad (1)$$

动量输运方程为

$$n_e m_e \left( \frac{\partial}{\partial t} + \mathbf{U}_e \cdot \nabla \right) \mathbf{U}_e = -en_e (\mathbf{E} + \mathbf{U}_e \times \mathbf{B}) - \nabla \mathbf{P}_e + n_e m_e \omega_e \mathbf{U}_e, \quad (2)$$

$$n_i m_i \left( \frac{\partial}{\partial t} + \mathbf{U}_i \cdot \nabla \right) \mathbf{U}_i = en_i (\mathbf{E} + \mathbf{U}_i \times \mathbf{B}) - \nabla \mathbf{P}_i + n_i m_i \omega_i \mathbf{U}_i. \quad (3)$$

$\omega_e$  和  $\omega_i$  分别是电子碰撞的有效角频率和氢离子碰撞的有效角频率.

麦克斯韦方程为

$$\nabla \cdot \mathbf{E} = \frac{1}{\varepsilon_0} \sum_\alpha e(n_\alpha - n_e) = 0, \quad (4)$$

$$\nabla \times \mathbf{E} = -\frac{\partial \mathbf{B}}{\partial t}, \quad (5)$$

$$\nabla \cdot \mathbf{B} = 0, \quad (6)$$

$$\nabla \times \mathbf{B} = \varepsilon_0 \mu_0 \frac{\partial \mathbf{E}}{\partial t} + \mu_0 \sum_\alpha e(n_\alpha \mathbf{U}_\alpha - n_e \mathbf{U}_e). \quad (7)$$

无外场 ( $\mathbf{E}_0 = \mathbf{B}_0 = 0$ ) 时,假设扰动场和扰动电流(均为小量)与时间的关系呈谐波形式  $\mathbf{E}_1 = \mathbf{E}_1 e^{-i\omega t}$  和  $\mathbf{B}_1 = \mathbf{B}_1 e^{-i\omega t}$ ,由式(7)得

$$\begin{aligned} \nabla \times \mathbf{B}_1 &= -i\omega \varepsilon_0 \mu_0 \mathbf{E}_1 + \mu_0 \mathbf{J}_1 = \\ &= -i\omega \varepsilon_0 \mu_0 \mathbf{E}_1 + \mu_0 \sigma \mathbf{E}_1 = \\ &= -i\omega \mu_0 \varepsilon_0 \left( 1 + i \frac{\sigma}{\varepsilon_0 \omega} \right) \mathbf{E}_1 = -i\omega \mu_0 \varepsilon \mathbf{E}_1. \end{aligned} \quad (8)$$

这里,  $\varepsilon = \varepsilon_0 \left( 1 + i \frac{\sigma}{\varepsilon_0 \omega} \right)$  为介电张量. 在没有稳态场和按时间平均的速度为零的简单情况下,对于稳态附近的小扰动,有

$$n_\alpha = n_{\alpha 0} + n_{\alpha 1}(\mathbf{x}) e^{-i\omega t}, \quad (9)$$

$$\mathbf{U}_\alpha = \mathbf{U}_{\alpha 1}(\mathbf{x}) e^{-i\omega t}, \quad (10)$$

$$\mathbf{E} = \mathbf{E}_1(\mathbf{x}) e^{-i\omega t}, \quad (11)$$

$$\mathbf{B} = \mathbf{B}_1(\mathbf{x}) e^{-i\omega t}, \quad (12)$$

则动量输运方程(2)和(3)变为

$$n_e m_e \frac{\partial \mathbf{U}_e}{\partial t} = -en_e (\mathbf{E} + \mathbf{U}_e \times \mathbf{B}) + n_e m_e \omega_e \mathbf{U}_e \Rightarrow$$

$$-i\omega \mathbf{U}_{e1} = -\frac{e}{m_e} \mathbf{E}_1 + \omega_e \mathbf{U}_{e1}, \quad (13)$$

$$n_i m_i \frac{\partial \mathbf{U}_i}{\partial t} = en_i (\mathbf{E} + \mathbf{U}_i \times \mathbf{B}) + n_i m_i \omega_i \mathbf{U}_i \Rightarrow$$

$$-i\omega \mathbf{U}_{i1} = \frac{e}{m_i} \mathbf{E}_1 + \omega_i \mathbf{U}_{i1}. \quad (14)$$

由式(13)、(14),可得

$$\mathbf{U}_{e1} = \frac{\left( \frac{e}{m_e} \right) \mathbf{E}_1}{i(\omega - i\omega_e)}, \quad \mathbf{U}_{i1} = \frac{-\left( \frac{i}{m_i} \right) \mathbf{E}_1}{i(\omega - i\omega_i)}. \quad (15)$$

根据麦克斯韦方程

$$\nabla \times \mathbf{B} = \varepsilon_0 \mu_0 \frac{\partial \mathbf{E}}{\partial t} + \mu_0 \mathbf{J} \Rightarrow$$

$$\nabla \times \mathbf{B}_1 = -i\omega \varepsilon_0 \mu_0 \mathbf{E}_1 + \mu_0 \sum_\alpha e(n_\alpha \mathbf{U}_{\alpha 1} - n_e \mathbf{U}_{e1}). \quad (16)$$

由式(15)、(16)和(8)可得

$$\begin{aligned} \varepsilon &= \varepsilon_0 \varepsilon_\gamma = \varepsilon_0 (\varepsilon'_\gamma + i\varepsilon''_\gamma) = \\ &= \varepsilon_0 \left[ 1 - \left( \frac{\omega_{pe}^2}{\omega(\omega - i\omega_e)} + \frac{\omega_{pi}^2}{\omega(\omega - i\omega_i)} \right) \right] = \\ &= \varepsilon_0 \left[ 1 - \left( \frac{\omega_{pe}^2}{\omega^2 + \omega_e^2} + \frac{\omega_{pi}^2}{\omega^2 + \omega_i^2} - \right. \right. \\ &\quad \left. \left. i \left( \frac{\omega_e \omega_{pe}^2}{\omega(\omega^2 + \omega_e^2)} + \frac{\omega_i \omega_{pi}^2}{\omega(\omega^2 + \omega_i^2)} \right) \right) \right]. \end{aligned} \quad (17)$$

$$\text{式(17)中, } \omega_{pe} = \sqrt{\frac{n_e e^2}{\varepsilon_0 m_e}}, \omega_{pi} = \sqrt{\frac{n_i e^2}{\varepsilon_0 m_i}}.$$

利用  $\nu = \frac{\omega}{2\pi}$ ,则单壁碳纳米管中氢等离子体因碰撞损耗电磁波的大小与入射电磁波频率  $\nu$ 、电子碰撞有效频率  $\nu_e$  和离子碰撞有效频率  $\nu_i$  的关系可通过其等效复介电常数表示为

$$\begin{aligned} \varepsilon &= \varepsilon_0 \left[ 1 - \left( \frac{\nu_{pe}^2}{\nu^2 + \nu_e^2} + \frac{\nu_{pi}^2}{\nu^2 + \nu_i^2} - \right. \right. \\ &\quad \left. \left. i \left( \frac{\nu_e}{\nu} \frac{\nu_{pe}^2}{\nu^2 + \nu_e^2} + \frac{\nu_i}{\nu} \frac{\nu_{pi}^2}{\nu^2 + \nu_i^2} \right) \right) \right]. \end{aligned} \quad (18)$$

## 2 铁催化高压歧化生成的单壁碳纳米管中氢等离子体的微波衰减系数

由于单壁碳纳米管中氢等离子体的相互碰撞,电磁波在氢等离子体中的波数可以用复数表示为

$$k = k_0 \sqrt{\frac{\varepsilon}{\varepsilon_0}} = k' + ik'', \quad k_0 = \frac{w}{c}. \quad (19)$$

根据电磁波在耗散介质中的传播原理,波数  $k$  的实部  $k'$  代表波在等离子体传播空间的变化,而虚部  $k''$  则表示波在等离子体传播过程中的损耗.

由式(18)和(19)可得

$$k' = \frac{2\pi\nu}{c} \left[ 1 + \frac{\nu_{pe}^2(\nu^2 + \nu_i^2)(\nu_{pe}^2 - 2\nu^2) + \nu_{pi}^2(\nu^2 + \nu_e^2)(\nu_{pi}^2 - 2\nu^2) + 2\nu_{pe}^2\nu_{pi}^2(\nu^2 + \nu_e\nu_i)}{\nu^2(\nu^2 + \nu_e^2)(\nu^2 + \nu_i^2)} \right]^{\frac{1}{4}} \cos \frac{\theta}{2}, \quad (20)$$

$$k'' = \frac{2\pi\nu}{c} \left[ 1 + \frac{\nu_{pe}^2(\nu^2 + \nu_i^2)(\nu_{pe}^2 - 2\nu^2) + \nu_{pi}^2(\nu^2 + \nu_e^2)(\nu_{pi}^2 - 2\nu^2) + 2\nu_{pe}^2\nu_{pi}^2(\nu^2 + \nu_e\nu_i)}{\nu^2(\nu^2 + \nu_e^2)(\nu^2 + \nu_i^2)} \right]^{\frac{1}{4}} \sin \frac{\theta}{2}. \quad (21)$$

$$\text{其中 } \theta = \arctan \left\{ \frac{\nu_e\nu_{pe}^2(\nu^2 + \nu_i^2) + \nu_i\nu_{pi}^2(\nu^2 + \nu_e^2)}{[(\nu^2 + \nu_e^2)(\nu^2 + \nu_i^2) - \nu_{pe}^2(\nu^2 + \nu_i^2) - \nu_{pi}^2(\nu^2 + \nu_e^2)]\nu} \right\}$$

微波等离子体中自由电子密度和氢离子密度是相等的,即  $n_e = n_i$ , 数量级一般在  $10^{17} \sim 10^{19} \text{ m}^{-3}$  之间<sup>[15]</sup>. 考虑到碳纳米管对氢气的吸附量以及微波作用后氢形成等离子体的数量和比率,  $n_e$  取  $10^{17} \text{ m}^{-3}$  数量级.  $\nu_e$  和  $\nu_i$  可由统计理论推算, 是粒子密度和温度的函数, 且  $\nu_e = \nu_i$ , 实际应用时可取经验值. 对于非磁等离子体来说,  $\nu_e$  一般在  $10^9 \sim 10^{11} \text{ Hz}$  之间<sup>[16]</sup>. 考

虑到  $\frac{\omega_{pi}^2}{\omega_{pe}^2} = \frac{m_e}{m_i} = \frac{1}{1836}$ , 即  $\omega_{pi}^2 = \frac{1}{1836}\omega_{pe}^2$ .

微波衰减系数可用电磁波的波数虚部  $k''$  表示为

$$C_{\text{ma}} = 10\lg \left[ \frac{P(x)}{P_0} \right] = 10\lg \left[ \frac{E^2(x)}{E_0^2} \right] = 20(\lg e)k''. \quad (22)$$

假设取  $n_e = 2.150 \times 10^{17} \text{ m}^{-3}$ , 当  $\nu_e$  分别为 20.0、22.0 和 24.0 GHz 时, 由式(22)计算得到的单壁碳纳米管薄膜中氢等离子体在 0.2 ~ 18.0 GHz 频率范围内的微波衰减系数如图 1 所示.  $\nu_e$  分别为 20.0、22.0 和 24.0 GHz 时, 其对应的衰减峰频率分别为 2.46、2.45 和 2.44 GHz, 相应的衰减峰值分别是 78.079、71.089 和 65.24 dB/cm, 即随着电子碰撞有效频率  $\nu_e$  的增加, 微波衰减系数减小, 且衰减峰略向低频方向移动.

$\nu_e = 22.0 \text{ GHz}$ , 当  $n_e$  分别为  $2.050 \times 10^{17}$ 、 $2.150 \times 10^{17}$  和  $2.250 \times 10^{17} \text{ m}^{-3}$  时, 单壁碳纳米管薄膜中氢等离子体在 0.2 ~ 18.0 GHz 频率范围内的微波衰减系数如图 2 所示.  $n_e$  从  $2.050 \times 10^{17} \text{ m}^{-3}$  增加到  $2.250 \times 10^{17} \text{ m}^{-3}$  时, 衰减峰值从 67.806 dB/cm 增加到 74.371 dB/cm, 最大衰减频率则从 2.42 GHz 增加到 2.49 GHz, 即随着  $n_e$  的增加, 衰减峰向高频方向移动, 且微波衰减系数增大. 模拟结果表明, 2.45 GHz 附近频段的微波在单壁碳纳米管薄膜氢等离子体中具有很大的吸收衰减系数. 理论结果与文献<sup>[5-7]</sup>的实验现象一致.

### 3 结论

本文同时考虑了单壁碳纳米管中氢等离子体的电子碰撞和氢离子碰撞对微波损耗的影响, 构建了单

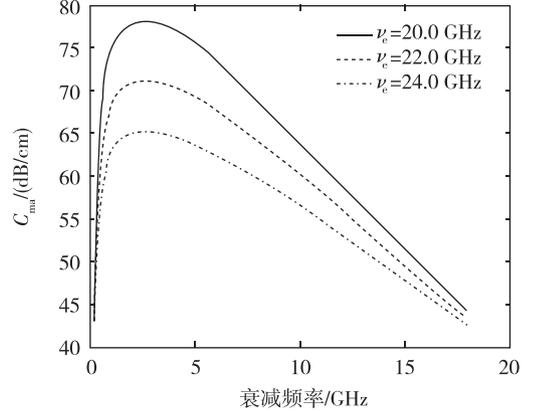


图 1  $n_e = 2.150 \times 10^{17} \text{ m}^{-3}$ ,  $\nu_e$  取不同值时, 单壁碳纳米管薄膜中氢等离子体的微波衰减系数  
Fig. 1 Microwave attenuation coefficient of hydrogen plasma via  $\nu$  in SCNTs film for different  $\nu_e$  at  $n_e = 2.150 \times 10^{17} \text{ m}^{-3}$

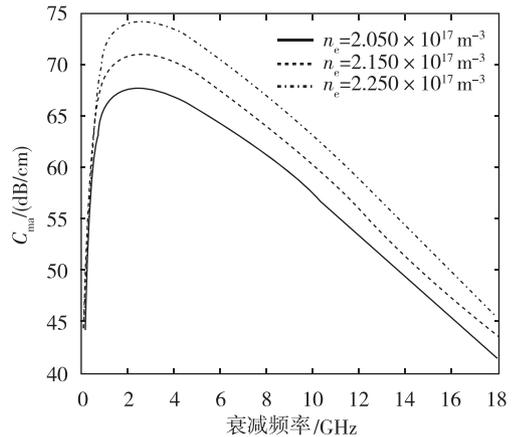


图 2  $\nu_e = 22.0 \text{ GHz}$ ,  $n_e$  取不同值时, 碳纳米管薄膜低温氢等离子体的微波衰减系数  
Fig. 2 Microwave attenuation coefficient of hydrogen plasma via  $\nu$  in SCNTs film for different  $n_e$  at  $\nu_e = 22.0 \text{ GHz}$

壁碳纳米管中氢等离子体微波损耗的理论模型. 计算结果显示, 铁催化高压歧化生成的单壁碳纳米管中氢等离子体对 2.45 GHz 微波产生强烈的损耗吸收, 其中电子碰撞是微波损耗吸收的主要原因, 氢离子碰撞对微波损耗吸收的影响不是很大.

## 参考文献

## References

- [ 1 ] 彭志华,彭景翠,欧玉,等.碳纳米管微波损耗机理的探讨[J].功能材料,2006,37(4):621-623  
PENG Zhihua, PENG Jingcui, OU Yu, et al. Study on carbon nanotubes microwave loss mechanism[J]. Journal of Functional Materials, 2006, 37(4): 621-623
- [ 2 ] Peng Z H, Peng J C, Peng Y F, et al. Complex permittivity and microwave absorption properties of carbon nanotubes/polymer composite: A numerical study[J]. Physics Letter A, 2008, 372(20): 3714-3718
- [ 3 ] Peng Z H, Peng J C, Peng Y F, et al. Complex conductivity and permittivity of single wall carbon nanotubes/polymer composite at microwave frequencies: A theoretical estimation[J]. Chinese Science Bulletin, 2008, 53(22): 3497-3504
- [ 4 ] Imholt T J, Dyke C A, Hasslacher B, et al. Nanotubes in microwave fields: Light emission, intense heat, outgassing, and reconstruction[J]. Chem Mater, 2003, 15(21): 3969-3970
- [ 5 ] Wadhawan A, Garrett D, Perez J M. Nanoparticle-assisted microwave absorption by single-wall carbon nanotubes[J]. Applied Physics Letters, 2003, 83(13): 2683-2685
- [ 6 ] Naab F, Dhoubhadel M, Holland O W, et al. The role of metallic impurities in the interaction of carbon nanotubes with microwave radiation[C]//Proceedings of the 10th International Conference on Particle Induced X-ray Emission and its Analytical Applications, Portoroz, Slovenia, 2004, 601:1-4
- [ 7 ] Anand A, Roberts J A, Naab F, et al. Select gas absorption in carbon nanotubes loading a resonant cavity to sense airborne toxin gases[J]. Nuclear Instruments and Methods in Physics Research Section B: Beam Interactions with Materials and Atoms, 2005, 241(1/2/3/4): 511-516
- [ 8 ] Ye Z, Deering W D, Krokhin A, et al. Microwave absorption by an array of carbon nanotubes: A phenomenological model[J]. Phys Rev B, 2006, 74(7): 075425(1)-075425(5)
- [ 9 ] 郭燕春,彭志华,彭延峰,等.碳纳米管低温氢等离子体的微波吸收特性研究[J].低温物理学报,2011,33(6): 454-457  
GUO Yanchun, PENG Zhihua, PENG Yanfeng, et al. Investigation on microwave absorbing properties of cold hydrogen plasma in carbon nanotube[J]. Chinese Journal of Low Temperature Physics, 2011, 33(6): 454-457
- [ 10 ] Kajiura H, Tsutsui S, Kadono K, et al. Hydrogen storage capacity of commercially available carbon materials at room temperature[J]. Applied Physics Letters, 2003, 82(7): 1105-1107
- [ 11 ] Lawrence J, Xu G. High pressure saturation of hydrogen stored by single-wall nanotubes[J]. Applied Physics Letters, 2004, 84(6): 918-920
- [ 12 ] Pradhan B K, Harutyunyan A R, Eklund P C, et al. Hydrogen storage on HiPCO SWNTs[C]//American Physical Society, Annual APS March Meeting, 2002, Indianapolis, Indiana Meeting ID: MAR02, Abstract #U25. 011
- [ 13 ] Baldwin D E. Kinetic model of Tonks-Dattner resonances in plasma columns[J]. Phys Fluids, 1969, 12(2): 279-290
- [ 14 ] Sauer K, Bogdanov A, Baumgärtel K. The protonopause-an ion composition boundary in the magnetosheath of comets, Venus and Mars[J]. Advances in Space Research, 1995, 16(4): 153-158
- [ 15 ] Toi K, Ikeda R, Takeuchi M, et al. Experimental simulation of high temperature plasma transport using almost dimensionally similar cold plasmas in the compact helical system[J]. Journal of Plasma and Fusion Research Series, 2004, 6: 516-518
- [ 16 ] Akhtar K, Scharer J E, Tysk S M, et al. Plasma interferometry at high pressures[J]. Review of Scientific Instruments, 2003, 74(2): 996-1001

## Investigation on microwave attenuation mechanisms of hydrogen plasma in HiPco single wall carbon nanotubes

GUO Yanchun<sup>1</sup> PENG Zhihua<sup>1</sup> CHEN You<sup>1</sup> JIA Peng<sup>1</sup> PENG Yanfeng<sup>1</sup> NING Yantao<sup>1</sup> GUO Ping<sup>1</sup>

<sup>1</sup> School of Mathematics and Physics, University of South China, Hengyang 421001

**Abstract** Using double-fluid theory, a microwave attenuation coefficient of hydrogen plasma in Single Wall Carbon Nanotubes (SCNTs), which were grown by iron-catalyzed high-pressure disproportionation (HiPco), is deduced theoretically. In this paper, both the electron collision absorption and ion collision absorption of hydrogen plasma in SCNTs are considered in detail. Under different conditions, microwave attenuation coefficient is calculated theoretically in the frequency range of 0.2 – 18 GHz. The simulation results show that hydrogen plasma in HiPco SCNTs exhibits strong microwave (around 2.45 GHz) absorption. The numerical results are in good agreement with the experimental data.

**Key words** single wall carbon nanotubes; hydrogen plasma; complex dielectric constant; microwave attenuation